

Manuscript Number: JCLEPRO-D-19-05319R2

Title: Rapid sintering of weathered municipal solid waste incinerator bottom ash and rice husk for lightweight aggregate manufacturing and product properties

Article Type: Original article

Keywords: Lightweight aggregate; weathered incinerator bottom ash; residual agricultural biomass; rice husk

Corresponding Author: Dr. Josep Maria Ma. Chimenos, Ph.D.

Corresponding Author's Institution: University of Barcelona

First Author: Jessica Giro-Paloma

Order of Authors: Jessica Giro-Paloma; Jofre Mañosa; Àlex Maldonado-Alameda; Margarida J Quina; Josep Maria Ma. Chimenos, Ph.D.

Abstract: This study assessed the technical feasibility of formulating lightweight aggregates (LWA) from municipal solid waste incinerator bottom ash (IBA) and residual biomass. Weathered IBA (WIBA) particles larger than 8 mm contain a mixture of calcium-rich compounds and other silicates mainly composed of glass and synthetic and natural ceramics, with low contents of heavy metals and soluble salts. Unfired LWA were formulated with the particle size fraction of WIBA larger than 8 mm and rice husk (RH) used as the bloating agent. Rapid sintering of the unfired spherical pellets at 1,100°C for 5 min produced some cohesive sintered LWA, whose porosity, apparent particle density, water absorption, and compressive strength directly correlated with the percentage of RH added. The fired LWA formulated with 5 wt.% of RH showed the highest bloating index (115%) and porosity (53%) and the lowest apparent particle density (0.61 Mg·m<sup>-3</sup>) and compressive strength (1.4 MPa). The addition of more than 5 wt.% of RH increased the internal temperature of the sintered aggregates and decreased the viscosity of the molten glassy materials, resulting in the collapse of the inner structure. Consequently the porosity decreased and the apparent density of the particles increased, thereby shrinking the volume of the fired LWA. According to the standard leaching test (EN 12457-4), both the unfired precursor and the sintered aggregates showed concentrations of heavy metals and metalloids in the leachates that were well below the safety limits established for their reuse as secondary materials.

# Rapid sintering of weathered municipal solid waste incinerator bottom ash and rice husk for lightweight aggregate manufacturing and product properties

J. Giro-Paloma<sup>a</sup>, J. Mañosa<sup>a</sup>, A. Maldonado-Alameda<sup>a</sup>, M.J. Quina<sup>b</sup>, J.M. Chimenos<sup>a,\*</sup>

<sup>a</sup> Departament de Ciència de Materials i Química Física, Universitat de Barcelona, C/ Martí i Franquès 1, 08028, Barcelona, Spain.

<sup>b</sup> CIEPQPF- Chemical Process Engineering and Forest Products Research Centre, Department of Chemical Engineering, University of Coimbra, Rua Sílvio Lima, Coimbra, 3030-790, Portugal

\* Corresponding author e-mail: [chimenos@ub.edu](mailto:chimenos@ub.edu)

Ref. No.: **JCLEPRO-D-19-05319R1**

Title: **Rapid sintering of weathered municipal solid waste incinerator bottom ash and rice husk for lightweight aggregate manufacturing and product properties**

**Answers to the reviewer:**

First of all, the authors would like to thank the Editor and Reviewers for all the corrections and suggestions. We have considered them to enhance the quality of our manuscript. The responses to the reviewer's comments and questions are presented below. We hope we have answered all the questions and clarified all the issues.

**Answers to Reviewer #2**

- 1. Suggested title: Rapid sintering of weathered municipal solid waste incinerator bottom ash and rice husk for lightweight aggregate manufacturing and product properties**

Done. The title has been changed according to the suggestion.

- 2. A notation list is necessary.**

A section with the nomenclature has been added before to the introduction.

- 3. The broken reference linkage in Page 12, Line 30 has still not been deleted.**

The linkage has been deleted.

**Answers to Reviewer #3:**

**There is a remaining linkage error on page 12, line 30. Such broken links are very common after managing the manuscript for submission, and only after printing (for example, pdf printing) it can be noticed. I recommend the pdf printing and double checking before the submission to avoid inconveniences.**

Done. The pdf file has been checked before the submission.

1  
2  
3  
4  
5  
6  
7  
8  
9  
10  
11  
12  
13  
14  
15  
16  
17  
18  
19  
20  
21  
22  
23  
24  
25  
26  
27  
28  
29  
30  
31  
32  
33  
34  
35  
36  
37  
38  
39  
40  
41  
42  
43  
44  
45  
46  
47  
48  
49  
50  
51  
52  
53  
54  
55  
56  
57  
58  
59  
60  
61  
62  
63  
64  
65

# Rapid sintering of weathered municipal solid waste incinerator bottom ash and rice husk for lightweight aggregate manufacturing and product properties

J. Giro-Paloma<sup>a</sup>, J. Mañosa<sup>a</sup>, A. Maldonado-Alameda<sup>a</sup>, M.J. Quina<sup>b</sup>, J.M. Chimenos<sup>a,\*</sup>

<sup>a</sup> Departament de Ciència de Materials i Química Física, Universitat de Barcelona, C/ Martí i Franquès 1, 08028, Barcelona, Spain.

<sup>b</sup> CIEPQPF- Chemical Process Engineering and Forest Products Research Centre, Department of Chemical Engineering, University of Coimbra, Rua Sílvio Lima, Coimbra, 3030-790, Portugal

\* Corresponding author e-mail: [chimenos@ub.edu](mailto:chimenos@ub.edu)

1  
2 **Abstract**  
3

4 This study assessed the technical feasibility of formulating lightweight aggregates (LWA) from  
5 municipal solid waste incinerator bottom ash (IBA) and residual biomass. Weathered IBA (WIBA)  
6 particles larger than 8 mm contain a mixture of calcium-rich compounds and other silicates mainly  
7 composed of glass and synthetic and natural ceramics, with low contents of heavy metals and soluble  
8 salts. Unfired LWA were formulated with the particle size fraction of WIBA larger than 8 mm and  
9 rice husk (RH) used as the bloating agent. Rapid sintering of the unfired spherical pellets at 1,100°C  
10 for 5 min produced some cohesive sintered LWA, whose porosity, apparent particle density, water  
11 absorption, and compressive strength directly correlated with the percentage of RH added. The fired  
12 LWA formulated with 5 wt.% of RH showed the highest bloating index (115%) and porosity (53%)  
13 and the lowest apparent particle density ( $0.61 \text{ Mg}\cdot\text{m}^{-3}$ ) and compressive strength (1.4 MPa). The  
14 addition of more than 5 wt.% of RH increased the internal temperature of the sintered aggregates and  
15 decreased the viscosity of the molten glassy materials, resulting in the collapse of the inner structure.  
16 Consequently the porosity decreased and the apparent density of the particles increased, thereby  
17 shrinking the volume of the fired LWA. According to the standard leaching test (EN 12457-4), both  
18 the unfired precursor and the sintered aggregates showed concentrations of heavy metals and  
19 metalloids in the leachates that were well below the safety limits established for their reuse as  
20 secondary materials.  
21  
22  
23  
24  
25  
26  
27  
28  
29  
30  
31  
32  
33  
34  
35  
36  
37  
38

39 *Keywords:* Lightweight aggregate; weathered incinerator bottom ash; residual agricultural biomass;  
40 rice husk.  
41  
42  
43  
44  
45  
46  
47  
48  
49  
50  
51  
52  
53  
54  
55  
56  
57  
58  
59  
60  
61  
62  
63  
64  
65

## Nomenclature

<i>APC</i>	air pollution control fly ash
<i>BI</i>	bloating index
<i>DTG</i>	derivative of the thermogravimetric
<i>IBA</i>	incinerator bottom ash
<i>ICP-MS</i>	inductively coupled plasma mass spectrometry
<i>LOI</i>	loss on ignition
<i>LWA</i>	lightweight aggregates
<i>MSW</i>	municipal solid waste
<i>RH</i>	rice husk
<i>RHA</i>	rice husk ash
<i>TGA</i>	thermogravimetric analysis
<i>WIBA</i>	weathered incinerator bottom ash
<i>XRD</i>	X-Ray diffraction
<i>XRF</i>	X-ray fluorescence
$\sigma_c$	compressive strength

## 1. Introduction

Due to the growing amount of residual waste in Europe, the Waste Framework Directive (2008/98/EC), amended by Directive (EU) 2018/851, encourages to apply the waste hierarchy to provide viable alternatives for managing waste and efficiently use resources to move towards a low-carbon economy. This includes the development of sustainable alternatives that can reuse different kinds of waste by formulating them into secondary materials.

1  
2  
3  
4  
5  
6  
7  
8  
9  
10  
11  
12  
13  
14  
15  
16  
17  
18  
19  
20  
21  
22  
23  
24  
25  
26  
27  
28  
29  
30  
31  
32  
33  
34  
35  
36  
37  
38  
39  
40  
41  
42  
43  
44  
45  
46  
47  
48  
49  
50  
51  
52  
53  
54  
55  
56  
57  
58  
59  
60  
61  
62  
63  
64  
65

Incineration of municipal solid waste (MSW) in waste-to-energy plants is expected to increase all over the world due to increased consumption and the limited use of landfills (Cabrera et al., 2016). Although the incineration process considerably reduces the mass and volume of MSW by about 75% and 90%, respectively, it still produces significant amounts of ash, namely incinerator bottom ash (IBA) and air pollution control (APC) fly ash (Wiles, 1995). IBA is the most significant waste from MSWI, accounting for 85-95% of the solid remaining from combustion (Izquierdo et al., 2002). It is classified as non-hazardous waste (EWC 190112) and can be revalorized as secondary raw material after weathering for 2-3 months to immobilize heavy metals (Chimenos et al., 1999; Grosso et al., 2011).

IBA is a highly heterogeneous material, mainly composed of glass, synthetic and natural ceramics, magnetic and paramagnetic metals, and a small percentage of unburned organic matter (Chimenos et al., 1999). Glass (primary and secondary glass) is the major component (40-60 %), while both synthetic ceramics and mineral compounds account for more than 30% (del Valle-Zermeño et al., 2017).. However, the distribution of these materials is not homogeneous and depends on the particle size. While the finer fractions contain most of the heavy metals and soluble salts, the coarser fractions are rich in glass cullet and synthetic ceramics, like pieces of bricks, porcelain or tiles. Accordingly, IBA is regarded as a mixture of calcium-rich compounds and other silicates enriched in iron and sodium (Freyssinet et al., 2002), with appropriate chemical and physical characteristics for reuse as secondary materials in civil engineering and construction (Verbinnen et al., 2016). Though, the reuse of IBA as secondary material may be limited by its high levels of heavy metals, chlorides and sulphates, which mainly occur in IBA particle size fraction lower than 4 mm and can be mobilized in the aqueous phase by leaching process (Chimenos et al., 2003; del Valle-Zermeño et al., 2014).

Sintering at high temperatures has been shown to significantly reduce the release of heavy metals, which are incorporated or embedded into the neo-formed crystalline or vitreous phases (Bourtsalas et

1 al., 2015; Schabbach et al., 2012; Verbinnen et al., 2016). Although the leaching potential  
2 appreciably decreases as the processing temperature increases, the sintering of IBA at temperatures  
3 of around 1,100 °C, to obtain lightweight aggregates (LWA) for instance, reduces the release of  
4 heavy metals when compared to the original unbound material (Cheeseman et al., 2005, 2003).  
5  
6  
7  
8  
9

10 LWA, which have very low densities ( $0.5-2.0 \text{ g}\cdot\text{cm}^{-3}$ ), are being increasingly used to formulate  
11 lightweight concrete, lightweight geotechnical fills, insulation products, soil engineering, hydro-  
12 culture, drainage, roof gardens, and filters, among others (Cheeseman et al., 2005; Quina et al.,  
13 2014). In addition, LWA display acoustic insulation and fire resistance and have a low thermal  
14 conductivity (Qiao et al., 2008). Besides naturally occurring low-density materials (e.g. volcanic  
15 cinders or pumice), LWA can be produced by thermal processes using raw materials with expansive  
16 properties, such as clayey materials. LWA can also be manufactured from industrial by-products  
17 such as fly ash from coal power plants, sewage sludge or expanded blast-slag (Cheeseman et al.,  
18 2005; González-Corrochano et al., 2012, 2009; Kourti and Cheeseman, 2010). Furthermore, the use  
19 of MSWI waste, mainly APC fly ash, to produce LWA has also been reported (Hwang et al., 2012;  
20 Quina et al., 2014; Tan et al., 2012). Thus, because of its high glass content (i.e. low softening point  
21 material) and the possibility to encapsulate the heavy metals contained, an attractive way to reuse  
22 IBA could be as a resource in the formulation of LWA (Cheeseman et al., 2005).  
23  
24  
25  
26  
27  
28  
29  
30  
31  
32  
33  
34  
35  
36  
37  
38  
39  
40  
41  
42

43 To achieve an appropriately expanded material, two conditions are necessary: the presence of  
44 substances that release gases at high temperatures and a plastic phase with adequate viscosity to trap  
45 the evolved gases. In this regard and to increase the porosity of the material to provide a lower  
46 density, biomass could be added since it decomposes during sintering to produce high volumes of  
47 gases, e.g., oil (Quina et al., 2014; Quina et al., 2014b), thereby facilitating the bloating before  
48 sintering. Regarding the possibility of adding biomass, rice husk (RH) could be used to increase  
49 porosity (Chiang et al., 2009), providing amorphous-Si to improve the cohesive forces between  
50 particles during sintering. RH is a major agricultural by-product comprising about 40% cellulose,  
51  
52  
53  
54  
55  
56  
57  
58  
59  
60  
61  
62  
63  
64  
65



1  
2  
3  
4  
5  
6  
7  
8  
9  
10  
11  
12  
13  
14  
15  
16  
17  
18  
19  
20  
21  
22  
23  
24  
25  
26  
27  
28  
29  
30  
31  
32  
33  
34  
35  
36  
37  
38  
39  
40  
41  
42  
43  
44  
45  
46  
47  
48  
49  
50  
51  
52  
53  
54  
55  
56  
57  
58  
59  
60  
61  
62  
63  
64  
65

30% lignin and 20% silica (Posi et al., 2013). After combustion, the rice husk ash, RHA, is mainly composed of silica (> 90 %), most of which is amorphous, depending on the temperature as well as the duration of the calcination process (Chandrasekhar et al., 2006; Rashid and Frantz, 1992).

In this study, the particle size fraction greater than 8 mm of IBA was used as a matrix and RH as the biomass component to produce lightweight aggregates, by means of a rapid sintering process. Accordingly, the aim of this work was to formulate and produce (ball-shaped pellets) LWA from two different by-products. The physicochemical and mechanical properties of the LWA produced were evaluated, as well as their environmental impact due to the leaching process with water.

## **2. Materials and methods**

### **2.1. Incinerator bottom ash and rice husk**

IBA was collected from a waste-to-energy plant located in Tarragona (Spain). The feed stream treated in this incineration plant is mainly composed of household rubbish with a small input from commercial sources. Approximately 32,000 tons per year of IBA are produced in the incineration plant and further treated in a conditioned/revalorization process for the recovery of valuable metals. The IBA is then stockpiled in the open for at least three months to ensure the immobilization of heavy metals by weathering.

Around 100 kg of weathered IBA (WIBA) was taken from various stockpiles. After homogenization by quartering method (Komnitsas, 2011) and drying, WIBA was screened through an 8-mm sieve, with particles larger than 8 mm (34 wt.%) taken for use in this study and later quartered by a riffle-type sample splitter. After removing the metal components with a metal magnet (Nd; 0.485 T), subsamples were dried overnight at 105°C and dry ball milled with a Jaw Crusher BB 50 (RETSCH) for 2 to 3 h before being passed through an 80-µm sieve to produce a fine homogeneous powder suitable for sintering.

1 The rice husk (RH) used in this study was supplied by the agricultural cooperative of the Delta de  
2 l'Ebre (Tarragona, Spain). After homogenization, RH subsamples were dried overnight at 105°C and  
3  
4 milled in a rotary cutting mill before being passed through an 80-µm sieve to produce a fine  
5  
6 homogeneous powder suitable for use as an additive in the formulation of unfired spherical pellets.  
7  
8  
9

10 The characterization of WIBA and RH involved X-ray fluorescence (XRF) using a Philips  
11 Panalytical PW 2400 sequential X-ray fluorescence spectrometer. X-Ray diffraction (XRD) pattern,  
12  
13 using a Bragg–Brentano Siemens D-500 powder diffractometer device with CuKα radiation and  
14  
15 processing the data by the X'Pert Highscore software, and thermogravimetric analysis (TGA) and the  
16  
17 derivative of the TGA curve (DTG) in air atmosphere, using a TA Instruments SDT Q600, a heating  
18  
19 rate of 10°C min<sup>-1</sup> from 30 to 1,200°C and a flow rate of gas of 50 mL min<sup>-1</sup>.  
20  
21  
22  
23  
24  
25

## 26 **2.2. Production of lightweight aggregates**

27  
28

29 According to the designed proportions (Table 1), the resulting fine powders of WIBA and RH  
30  
31 were thoroughly mixed to ensure homogeneity. Subsequently, a controlled amount of water (20-  
32  
33 25%) was added to the mixture to give consistency and workability that would allow the formation  
34  
35 of unfired spherical pellets with a diameter of 10-12 mm. Fifteen to eighteen “green” spherical  
36  
37 pellets were handmade for each formulation to determine their chemical, physical and mechanical  
38  
39 parameters. The molded pellets were dried at 105°C in an oven for 24 h prior to firing in an electric  
40  
41 laboratory furnace. The dried pellets were sintered in the furnace over pre-drilled holes (Ø = 8 mm)  
42  
43 on a rigid ceramic fiber board (Kaowool) (20 mm x 80 mm x 150 mm) at a target temperature of  
44  
45 1,100 °C for 5 min, before being quenched in air. This temperature was selected because sintering  
46  
47 pre-tests performed at lower temperatures (e.g. 1,050 °C) resulted in weak and poorly cohesive  
48  
49 aggregates lacking in consistency, which were considered to be non-sintered. Moreover, sintering at  
50  
51 temperatures above 1,100 °C (or firing times greater than 5 min) resulted in melted particles without  
52  
53 a regular shape and/or high density, thus producing a collapsed structure. Therefore, 1,100 °C and 5  
54  
55  
56  
57  
58  
59  
60  
61  
62  
63  
64  
65

1 min were the sintering conditions used for all the formulations (Table 1). Although the sintering  
2 temperature (1,100 °C) is above the working point of soda-lime-silica glass (995 °C; 10<sup>4</sup> P), the rapid  
3 sintering process (5 min) requires a higher temperature and lower viscosity to allow for the cohesion  
4 of the matrix and the formation of pores. Accordingly, the study only focused on the effects of  
5 adding different amounts of RH on the physical and mechanical properties of the sintered LWA.  
6  
7  
8  
9  
10  
11  
12

### 13 **2.3 Characterization of sintered LWA**

14  
15

16 The different formulations were characterized to determine their physical, mechanical and  
17 chemical properties, which would then be used to determine the optimal formulation (WIBA/RH,  
18 wt./wt.%) for obtaining LWA. In this regard, XRD analysis was performed. Furthermore, weight loss  
19 after the firing process at 1,100°C, dry density (apparent specific gravity) and water absorption  
20 according to the EN 1097-6:2000 standard, as well as shrinking (or enlargement) and the  
21 compressive strength of the sintered handmade spherical balls were determined. Based on the mean  
22 diameters of the unfired and sintered spherical balls (measured by using a digital caliper at 4-5  
23 positions each) before and after sintering, the bloating index (BI) was determined with equation Eq.  
24  
25  
26  
27  
28  
29  
30  
31  
32  
33  
34  
35  
36 1,

$$37 \quad BI (\%) = \frac{V_i - V_f}{V_i} \times 100 \quad \text{Eq. 1.}$$

38  
39  
40  
41  
42

43 where  $V_f$  is the estimated volume (cm<sup>3</sup>) after sintering and  $V_i$  is the estimated volume before  
44 sintering.  
45  
46  
47  
48

49 The compressive strength ( $\sigma_c$ ) of the individual sintered LWA was measured using a universal  
50 testing machine Zwick Roell Zmart-PRO, equipped with a 10 kN load cell, using a loading rate of 2  
51 mm·min<sup>-1</sup>. The sintered spherical pellets were inserted between two parallel rigid surfaces, while the  
52 load to fracture was analyzed. The compressive strength of all the formulations was compared with  
53 Eq. 2 (Cheeseman et al., 2005),  
54  
55  
56  
57  
58  
59  
60  
61  
62  
63  
64  
65

$$\sigma_c = \frac{2.8 \cdot P_c}{\pi \cdot X^2} \quad \text{Eq. 2}$$

where  $X$  is the distance between the loading points (the diameter of the sphere) (mm) and  $P_c$  the fracture load (N).

Finally, the standard leaching test EN 12457-4 was undertaken to determine the potential release of heavy metals and metalloids from WIBA and LWA. The leaching procedure involves the extraction of the solids with deionized water at the L/S ratio of 10 L·kg<sup>-1</sup> for 24 h under agitation. The liquid was separated with a 0.45 µm pore membrane, and 15 elements were analyzed by inductively coupled plasma mass spectrometry (ICP-MS), Perkin Elmer Optima 3200 RL.

### 3. Results and discussion

#### 3.1. Characterization of WIBA and RH

Table 2 shows the chemical composition of the fraction of WIBA larger than 8 mm, which was determined by XRF. The major compounds were SiO<sub>2</sub> and CaO, likely related to the content of glass cullet and synthetic ceramics in the MSW. The contents of Fe<sub>2</sub>O<sub>3</sub> and Al<sub>2</sub>O<sub>3</sub> were also significant, with the former mainly related to the presence of unrecovered ferrous metals and the latter possibly from both non-ferrous metals and clay-based synthetic ceramics (del Valle-Zermeño et al., 2017). XRD spectra (not shown) allowed the identification of calcite CaCO<sub>3</sub>, quartz SiO<sub>2</sub>, hydroxylapatite Ca<sub>5</sub>(PO<sub>4</sub>)<sub>3</sub>(OH), dolomite CaMg(CO<sub>3</sub>)<sub>2</sub>, vaterite (CaCO<sub>3</sub>), albite calcian (Na<sub>0.84</sub>Ca<sub>0.16</sub>)Al<sub>1.16</sub>Si<sub>2.84</sub>O<sub>8</sub>, Akermanite Ca<sub>2</sub>(Mg<sub>0.75</sub>Al<sub>0.25</sub>)(Si<sub>1.75</sub>Al<sub>0.25</sub>O<sub>7</sub>), orthoclase KAlSi<sub>3</sub>O<sub>8</sub>, and calcium sulphate Ca(SO<sub>4</sub>) as major crystalline phases. However, given the high content of glass cullet in this size fraction, the highest content should be considered as corresponding to the amorphous phase.

TGA of WIBA (Fig. 1) indicates that the mass loss occurred in several steps, with a total decomposition of around 9% denoting the presence of unburned organic matter (exothermic reaction), carbonates and other hydroxides and hydrated salts (endothermic reactions) decomposing

1 with temperature. Accordingly, a high volume of gases was expected to contribute to the bloating  
2 before LWA sintering, while a large weight loss would increase porosity and reduce the densities of  
3 the sintered aggregates. Total weight loss (8.92 wt.% at 1,000°C) is consistent with the results  
4 reported in Table 2 (9.58 wt% of LOI at 1,000°C).  
5  
6  
7  
8  
9

10 Regarding the RH thermal degradation, TGA and DTG curves are depicted in Fig. 2. An initial  
11 weight loss occurred below 100°C, which was related to the vaporization of water because of the  
12 hydrophilic character of the lignocellulose fibers. The weight loss in the temperature range from 225  
13 to 550°C was due to the combustion of hemicellulose, lignin, pectin and cellulose (Johar et al., 2012).  
14 TGA analysis revealed a total decomposition of around 76%. On burning, the organic matter  
15 decomposed, generating a high volume of gases that again contributed to the bloating process and the  
16 increase in the porosity of the LWA samples, reducing the densities of the sintered aggregates.  
17  
18  
19  
20  
21  
22  
23  
24  
25  
26  
27

28 According to the XRF and XRD characterization, the major compound in the residual ash of RH  
29 was silica (SiO<sub>2</sub>, around 95%), which remains in the amorphous form at combustion temperatures of  
30 up to 900°C (Blissett et al., 2017; Faé Gomes et al., 2016; Yeoh et al., 1979).  
31  
32  
33  
34  
35

### 36 **3.2. Properties of LWA**

37  
38  
39

40 Six formulations were tested (Table 1) starting with unfired particles of 10-12 mm. As shown in  
41 Fig. 3, the sintered aggregates may exhibit bloating (enlargement of its diameter) or shrinking  
42 depending on the percentage of RH used in the formulation. Indeed, the weight loss of each unfired  
43 spherical pellet was determined after the sintering process to obtain their corresponding fired  
44 aggregates. Fig.4 depicts a good correlation ( $R^2=0.94$ ) between weight loss and the percentage of RH  
45 used in the different formulations. However, neither the weight loss of the WIBA fraction (5.4 wt.%;  
46 0 wt.% of RH) nor the weight loss of the RH (i.e. slope of the regression line;  $\approx 60$  wt.%)  
47 corresponded to the weight loss previously determined in the TGA of both sources (see Fig. 1 and 2).  
48  
49  
50  
51  
52  
53  
54  
55  
56  
57  
58  
59  
60  
61  
62  
63  
64  
65

1 process (e.g., the combustion of RH in anoxic conditions) or to the combination of some calcination  
2 products resulting in the formation of neo-formed mineral phases. Regarding the XRD analysis of the  
3 sintered LWA samples, wollastonite ( $\text{CaSiO}_3$ ) and quartz ( $\text{SiO}_2$ ) were the main crystalline phases  
4 detected for all the formulations studied, while the presence of carbonates or hydroxides (e.g. calcite)  
5 was not perceived. However, the highest content should be considered as corresponding to the  
6 vitreous phases.  
7  
8  
9  
10  
11  
12  
13  
14

15 During the firing process, the high volume of gases generated by the thermal decomposition of  
16 both WIBA and RH contributed to the bloating before sintering, thereby increasing porosity, with the  
17 weight loss reducing the densities of the sintered LWA.  
18  
19  
20  
21  
22

23 Moreover, it is also important to note that the expanded sintered specimens showed two different  
24 layers (Fig. 5): the vitrified outer layer on the external surface, and the vitreous skeleton inner layer.  
25 Both the porosity and pore size, as well as the colors of the inner and outer layers, were different and  
26 varied with the percentage of RH added. Fired LWA formulated using only WIBA (0 wt.% of RH;  
27 Fig. 5a) presented a homogeneous porous texture that consisted of small closed pores evenly  
28 distributed over all the sintered material. In this case, there were no major differences in the texture  
29 of the inner and outer layers, as well as in their pore sizes and color. The thermal decomposition of  
30 the carbonates and hydroxides in the WIBA (> 8 mm), distributed homogeneously throughout the  
31 material, was sufficient to generate a large number of pores.  
32  
33  
34  
35  
36  
37  
38  
39  
40  
41  
42  
43  
44  
45

46 The addition of 2 to 5 wt.% of RH (Fig. 5b and 5c, respectively) led to a sharp increase in the  
47 number of large pores in the inner layer, while the outer layer still showed tiny pores that were  
48 evenly distributed. In these cases (2 and 5 wt.% of RH), the increase in the percentage of RH used  
49 also increased the pore size, both in the inner and outer layer. However, the addition of 10 wt.% of  
50 RH (Fig. 5d) produced a compact texture in the inner layer, while the largest pores were concentrated  
51  
52  
53  
54  
55  
56  
57  
58  
59  
60  
61  
62  
63  
64  
65

1  
2  
3  
4  
5  
6  
7  
8  
9  
10  
11  
12  
13  
14  
15  
16  
17  
18  
19  
20  
21  
22  
23  
24  
25  
26  
27  
28  
29  
30  
31  
32  
33  
34  
35  
36  
37  
38  
39  
40  
41  
42  
43  
44  
45  
46  
47  
48  
49  
50  
51  
52  
53  
54  
55  
56  
57  
58  
59  
60  
61  
62  
63  
64  
65

in the outer layer. Finally, the addition of 15 wt.% of RH (Fig. 5e) generated a compact vitreous structure with the smallest pore sizes, both in the inner and outer layer.

With the exception of the sintered LWA in the absence of RH (0 wt.% of RH), the outer and inner layers showed noticeable differences in color, with the color gradually darkening with an increasing percentage of RH added. The darkening of the inner layer is attributable to the char particles generated during the anoxic combustion of the biomass (RH), while in the oxic conditions (outer layer) this combustion is complete and the dark color disappears.

Through a computer-based analysis (Image J<sup>TM</sup> processing program), the 2D cross-section images obtained by optical microscopy (e.g. Fig. 5a-e) were used to determine the porosity (Dullien, 1991) and distribution of pore sizes for each formulation of LWA. The resulting images were digitized directly from the microscope and the greyscale images were then thresholded to differentiate between the pore and solid spaces (i.e. the number of pore pixels), while the noise in the image was removed. As it is difficult to differentiate small pores in greyscale images, especially in samples with a darker inner layer, all pores smaller than 5  $\mu\text{m}$  were discarded during analysis. For all the formulations studied, the vast majority of pores were smaller than 50  $\mu\text{m}$  (Fig. 6a). However, with the addition of small percentages of RH (2 to 5 wt.%), the pore size increased significantly, increasing with the percentage of RH used and resulting in pores larger than 700  $\mu\text{m}$  (e.g., Fig. 5c). By contrast, with the addition of a higher percentage of RH (e.g. 10 to 15 wt.% of RH), large pores did not form and most of them were smaller than those formulated without RH or with only a small percentage of RH (i.e.  $\leq 5$  wt.% of RH). The highest percentage of large pores ( $> 350$   $\mu\text{m}$ ) was observed in sintered aggregates formulated with 5 wt.% of RH, while aggregates formulated with higher percentages of RH presented low number of large pores. Considering the area and sphericity factor of all the pores, calculated by an image computer-based analysis, porosity appeared to be a function of the percentage of the bloating agent used (Fig. 6b). However, due to the dark color of the inner layer of the fired LWA formulated with a higher percentage of RH (Fig. 5d and 5e), it is

1 possible that the porosity determined in these specimens was actually greater than the measurement  
2 obtained. However, the porosity of LWA did not increase with the percentage of added RH, reaching  
3 a maximum value of 54% when 5 wt.% of RH was utilized and then decreasing when the percentage  
4 of RH used was higher than 5 wt.%.  
5  
6  
7  
8  
9

10 Fig. 7 shows the bloating index, BI (%), as a function of the percentage of RH (wt.%) used, with  
11 negative values indicating bloating (enlargement) of the sintered LWA. In the absence of RH (0  
12 wt.% of RH), the sintering of WIBA particles larger than 8 mm caused a BI of approximately 26%.  
13 In this case, the gases generated during decarbonation and dehydration by the thermal decomposition  
14 of the WIBA were sufficient to expand the sintered aggregates. The BI increased with the percentage  
15 of RH, reaching a maximum when 5 wt.% of RH was used. The flue gases generated during the  
16 combustion of the biomass increased the bloating to up to 115% of the initial volume, with the glassy  
17 material reaching the pyroplastic state and the viscosity of the melted material is right to trap the  
18 released gases. In addition, gases generated from the RH had sufficient vapor pressure to increase the  
19 pore volume and expand the material (see Fig. 6).  
20  
21  
22  
23  
24  
25  
26  
27  
28  
29  
30  
31  
32  
33  
34  
35

36 The porous network of the aggregates began to collapse when the amount of RH was greater than  
37 5 wt.%. The inner structure collapsed and the sintered aggregates bloat less or even shrink when high  
38 percentages of RH were used, consequently leading to the production of dense granules. Indeed,  
39 LWA with 15 wt.% of RH show shrinking compared to the unfired pellets. However, the BI was not  
40 affected by increasing the percentage of RH from 15 wt.% (i.e. 20 wt.% of RH). In these cases, it is  
41 possible that the inner temperature increases significantly due to the combustion of a large amount of  
42 biomass, decreasing the pyroplastic viscosity of the melted glassy material and increasing the  
43 cohesion between the WIBA particles. Consequently, the porosity and pore size decrease (see Fig.  
44 5), with the pores becoming evenly distributed to produce aggregates with a higher density.  
45  
46  
47  
48  
49  
50  
51  
52  
53  
54  
55  
56  
57  
58  
59  
60  
61  
62  
63  
64  
65



1 The apparent particle density ( $\text{Mg}\cdot\text{m}^{-3}$ ) and water absorption (wt.%) of the fired LWA were  
2 measured using the Archimedes principle, according to EN 1097-6:2000. Fig. 8 shows the effect of  
3 adding RH (wt.%) on both physical properties. The apparent particle density of all the fired LWA  
4 formulated with WIBA ( $> 8$  mm) and RH (Fig. 8a) varied between 0.6 and  $1.8 \text{ Mg}\cdot\text{m}^{-3}$ . As expected,  
5 particle density directly correlated with the porosity of the sintered LWA, with lower apparent  
6 density when the porosity was higher (Fig. 6b). Once again, the aggregates formulated with 5 wt.%  
7 of RH had the lowest apparent particle density ( $0.61 \text{ Mg}\cdot\text{m}^{-3}$ ). It is interesting to observe that the  
8 fired LWA formulated with a large amount of RH ( $> 15$  wt.%) had a lower apparent particle density  
9 than those formulated without the RH. In these cases, the collapse of the inner structure caused the  
10 shrinking of the particles and increased the apparent particle density.  
11  
12  
13  
14  
15  
16  
17  
18  
19  
20  
21  
22  
23  
24

25 Fig. 8b shows the water absorption of the fired LWA in relation to the amount of RH used. Water  
26 absorption increased linearly with the amount of bloating agent added, from 1.7 wt.% of water for  
27 LWA formulated without RH to 16 wt.% for particles formulated with 15 wt.% of RH. Since water  
28 absorption is directly related to open porosity, it is thought that a higher percentage of RH generates  
29 a higher percentage of pores in the outer (surface) layer during the rapid firing process. In this case,  
30 the slope of the estimated regression line was 0.92. Hence, water absorption (wt.%) can be thought of  
31 as equivalent to the percentage of RH (wt.%) added as the bloating agent. All the formulations  
32 assessed in this study had lower water absorption than some commercial LWA described in the  
33 literature (Ayati et al., 2019; Quina et al., 2014), which is a very desirable physical property in the  
34 production of lightweight concrete.  
35  
36  
37  
38  
39  
40  
41  
42  
43  
44  
45  
46  
47  
48  
49

50 Fig. 9 shows the effect of the percentage of RH used on compressive strength. The average  
51 compressive strength decreased from 6.6 MPa for 0 wt.% of RH to its minimum value of 1.4 MPa for  
52 5 wt.% of RH. After this point, compressive strength increased slightly until reaching a plateau when  
53 the percentage of RH added was more than 10 wt.%. This physical property is also significantly  
54  
55  
56  
57  
58  
59  
60  
61  
62  
63  
64  
65

1 affected by porosity and the inner pore size. Thus, the greater the porosity and inner pore size is (i.e.  
2 lower density LWA), the lower the compressive strength.  
3  
4

### 5 **3.3 Leaching impact assessment**

6  
7

8  
9 Finally, to determine the potential environmental impact of formulating LWA with residual  
10 sources (i.e. WIBA > 8 mm), the standard leaching test EN 12457-4 was performed. Table 3 shows  
11 the results of this test in relation to the percentage of RH added as the bloating agent. To carry out  
12 the leaching test the broken aggregates (< 10 mm) from the mechanical compression tests were used.  
13  
14 Table 3 also shows the results for WIBA particles as received and after ground into particles with  
15 diameters less than 80- $\mu$ m powder. The pH of the WIBA was above 9.0, controlled by the formation  
16 of calcium carbonate (Chimenos et al., 2003). After sintering, the pH fell to values close to 7.8 due to  
17 the decomposition of the carbonates and the incorporation of calcium into the siliceous matrix.  
18  
19 Moreover, both the unfired and sintered aggregates released heavy metals and metalloids in the  
20 leachates well below the limits established for reuse as secondary materials. The small differences  
21 between the fired aggregates were more likely to be due to the heterogeneity of the WIBA than to the  
22 differences in the formulation of the unfired LWA. The release of As was slightly higher in the  
23 leachates from the sintered LWA than from those of the WIBA used as precursor, probably due to  
24 the decrease in pH and the leaching of the iron oxides hosting As in their lattice structure.  
25  
26  
27  
28  
29  
30  
31  
32  
33  
34  
35  
36  
37  
38  
39  
40  
41  
42  
43

## 44 **4. Conclusions**

45  
46

47 This study demonstrated the feasibility of obtaining lightweight aggregates from WIBA particle  
48 size fraction larger than 8 mm through a rapid sintering process, as a way to revalorizing this fraction  
49 of WIBA rich in vitreous materials. The addition of RH as a bloating agent increased the porosity  
50 and decreased the apparent particle density of the sintered LWA. However, while the use of small  
51 amounts of RH (< 5 wt.%) resulted in the bloating of the aggregates during sintering, the addition of  
52 more than 10 wt.% of RH produced shrinking and generated denser aggregates than those obtained  
53  
54  
55  
56  
57  
58  
59  
60  
61  
62  
63  
64  
65

1 without RH. In this case, the combustion of the large quantities of RH considerably increased the  
2 temperature, reducing the viscosity of the molten vitreous phases and causing the collapse of the  
3 internal structure.  
4  
5

6  
7  
8 All the physical properties evaluated were directly related to the porosity of the sintered LWA,  
9 which in turn could be controlled by adding different amounts of RH. The compressive strength and  
10 water absorption of the LWA obtained in this study were similar to or better than those of the  
11 commercial LWA described in the literature, therefore increasing the usability of these LWA. Large  
12 porosity generates low weight and good thermal and acoustic insulation. Therefore, the addition of  
13 RH is a promising method for regulating the porosity of LWA formulated with WIBA (> 8 mm).  
14  
15  
16  
17  
18  
19  
20  
21  
22

23 The use of weathered IBA, in particular the fraction larger than 8 mm containing lower  
24 concentrations of soluble salts, heavy metals, and metalloids, decreases the polluting potential of the  
25 precursor. Moreover, the formation of the outer vitreous layer waterproofs the inner layer and  
26 decreases the permeability to water, thereby reducing the release of pollutants.  
27  
28  
29  
30  
31  
32

### 33 **Acknowledgments**

34  
35  
36 The work was partially funded by the Spanish Government (BIA2017-83912-C2-1-R) and by an  
37 STSM Grant from COST Action CA15115. The authors would like to acknowledge the Catalan  
38 Government for the quality accreditation given to the research group DIOPMA (2017 SGR 118).  
39 Authors also thank SIRUSA and VECSA for supplying the MSWI bottom ash and the cooperative of  
40 the Delta de l'Ebre for the rice husk. Mr Alex Maldonado-Alameda is grateful to the Government of  
41 Catalonia for the research grant FI-DGR 2017.  
42  
43  
44  
45  
46  
47  
48  
49  
50

### 51 **References**

- 52  
53  
54 Ayati, B., Molineux, C., Newport, D., Cheeseman, C., 2019. Manufacture and performance of  
55 lightweight aggregate from waste drill cuttings. *J. Clean. Prod.* 208, 252–260.  
56 doi:<https://doi.org/10.1016/j.jclepro.2018.10.134>  
57  
58  
59 Blissett, R., Sommerville, R., Rowson, N., Jones, J., Laughlin, B., 2017. Valorisation of rice husks  
60 using a TORBED® combustion process. *Fuel Process. Technol.* 159, 247–255.  
61  
62  
63  
64  
65

doi:10.1016/j.fuproc.2017.01.046

- 1  
2 Bourtsalas, A., Vandeperre, L.J., Grimes, S.M., Themelis, N., Cheeseman, C.R., 2015. Production of  
3 pyroxene ceramics from the fine fraction of incinerator bottom ash. *Waste Manag.* 45, 217–225.  
4 doi:10.1016/j.wasman.2015.02.016  
5
- 6 Cabrera, M., Galvin, A.P., Agrela, F., Beltran, M.G., Ayuso, J., 2016. Reduction of leaching impacts  
7 by applying biomass bottom ash and recycled mixed aggregates in structural layers of roads.  
8 *Materials (Basel)*. 9, 1–21. doi:10.3390/ma9040228  
9
- 10 Chandrasekhar, S., Pramada, P.N., Majeed, J., 2006. Effect of calcination temperature and heating  
11 rate on the optical properties and reactivity of rice husk ash. *J. Mater. Sci.* 41, 7926–7933.  
12 doi:10.1007/s10853-006-0859-0  
13
- 14 Cheeseman, C.R., Makinde, A., Bethanis, S., 2005. Properties of lightweight aggregate produced by  
15 rapid sintering of incinerator bottom ash. *Resour. Conserv. Recycl.* 43, 147–162.  
16 doi:10.1016/j.resconrec.2004.05.004  
17
- 18 Cheeseman, C.R., Monteiro Da Rocha, S., Sollars, C., Bethanis, S., Boccaccini, A.R., 2003. Ceramic  
19 processing of incinerator bottom ash. *Waste Manag.* 23, 907–916. doi:10.1016/S0956-  
20 053X(03)00039-4  
21
- 22 Chiang, K.-Y., Chou, P.-H., Hua, C.-R., Chien, K.-L., Cheeseman, C., 2009. Lightweight bricks  
23 manufactured from water treatment sludge and rice husks. *J. Hazard. Mater.* 171, 76–82.  
24 doi:10.1016/j.jhazmat.2009.05.144  
25
- 26 Chimenos, J., Segarra, M., Fernández, M., Espiell, F., 1999. Characterization of the bottom ash in  
27 municipal solid waste incinerator. *J. Hazard. Mater.* 64, 211–222. doi:10.1016/S0304-  
28 3894(98)00246-5  
29
- 30 Chimenos, J.M., Fernández, A.I., Miralles, L., Segarra, M., Espiell, F., 2003. Short-term natural  
31 weathering of MSWI bottom ash as a function of particle size. *Waste Manag.* 23, 887–895.  
32 doi:S0956- 053X(03)00074-6  
33
- 34 del Valle-Zermeño, R., Chimenos, J.M., Giró-Paloma, J., Formosa, J., 2014. Use of weathered and  
35 fresh bottom ash mix layers as a subbase in road constructions: Environmental behavior  
36 enhancement by means of a retaining barrier. *Chemosphere* 117, 402–409.  
37 doi:10.1016/j.chemosphere.2014.07.095  
38
- 39 del Valle-Zermeño, R., Gómez-Manrique, J., Giro-Paloma, J., Formosa, J., Chimenos, J.M., 2017.  
40 Material characterization of the MSWI bottom ash as a function of particle size. Effects of glass  
41 recycling over time. *Sci. Total Environ.* 581–582. doi:10.1016/j.scitotenv.2017.01.047  
42
- 43 Dullien, F.A.L., 1991. *Porous Media. Fluid Transport and Pore Structure.* Academic Press, Inc.,  
44 London.  
45
- 46 Faé Gomes, G.M., Philipssen, C., Bard, E.K., Zen, L.D., De Souza, G., 2016. Rice husk bubbling  
47 fluidized bed combustion for amorphous silica synthesis. *J. Environ. Chem. Eng.* 4, 2278–2290.  
48 doi:10.1016/j.jece.2016.03.049  
49
- 50 Freyssinet, P., Piantone, P., Azaroual, M., Itard, Y., Clozel-Leloup, B., Guyonnet, D., Baubron, J.C.,  
51 2002. Chemical changes and leachate mass balance of municipal solid waste bottom ash  
52 submitted to weathering. *Waste Manag.* 22, 159–172.  
53  
54  
55  
56  
57  
58  
59  
60  
61  
62  
63  
64  
65

- 1 González-Corrochano, B., Alonso-Azcárate, J., Rodas, M., 2012. Effect of thermal treatment on the  
2 retention of chemical elements in the structure of lightweight aggregates manufactured from  
3 contaminated mine soil and fly ash. *Constr. Build. Mater.* 35, 497–507.  
4 doi:10.1016/j.conbuildmat.2012.04.061
- 5 González-Corrochano, B., Alonso-Azcárate, J., Rodas, M., 2009. Characterization of lightweight  
6 aggregates manufactured from washing aggregate sludge and fly ash. *Resour. Conserv. Recycl.*  
7 53, 571–581. doi:10.1016/j.resconrec.2009.04.008
- 8 Grosso, M., Biganzoli, L., Rigamonti, L., 2011. A quantitative estimate of potential aluminium  
9 recovery from incineration bottom ashes. *Resour. Conserv. Recycl.* 55, 1178–1184.
- 10 Hwang, C.-L., Bui, L.A.-T., Lin, K.-L., Lo, C.-T., 2012. Manufacture and performance of  
11 lightweight aggregate from municipal solid waste incinerator fly ash and reservoir sediment for  
12 self-consolidating lightweight concrete. *Cem. Concr. Compos.* 34, 1159–1166.  
13 doi:10.1016/j.cemconcomp.2012.07.004
- 14 Izquierdo, M., López-Soler, A., Ramonich, E. V, Barra, M., Querol, X., 2002. Characterisation of  
15 bottom ash from municipal solid waste incineration in Catalonia. *J. Chem. Technol. Biotechnol.*  
16 77, 576–583.
- 17 Johar, N., Ahmad, I., Dufresne, A., 2012. Extraction, preparation and characterization of cellulose  
18 fibres and nanocrystals from rice husk. *Ind. Crops Prod.* 37, 93–99.  
19 doi:10.1016/j.indcrop.2011.12.016
- 20 Komnitsas, K.A., 2011. Potential of geopolymer technology towards green buildings and sustainable  
21 cities. *Procedia Eng.* 21, 1023–1032. doi:10.1016/j.proeng.2011.11.2108
- 22 Kourti, I., Cheeseman, C.R., 2010. Properties and microstructure of lightweight aggregate produced  
23 from lignite coal fly ash and recycled glass. *Resour. Conserv. Recycl.* 54, 769–775.  
24 doi:10.1016/j.resconrec.2009.12.006
- 25 Posi, P., Teerachanwit, C., Tanutong, C., Limkamoltip, S., Lertnimoolchai, S., Sata, V.,  
26 Chindapasirt, P., 2013. Lightweight geopolymer concrete containing aggregate from recycle  
27 lightweight block. *Mater. Des.* 52, 580–586. doi:10.1016/j.matdes.2013.06.001
- 28 Qiao, X.C., Ng, B.R., Tyrer, M., Poon, C.S., Cheeseman, C.R., 2008. Production of lightweight  
29 concrete using incinerator bottom ash. *Constr. Build. Mater.* 22, 473–480.  
30 doi:10.1016/j.conbuildmat.2006.11.013
- 31 Quina, M.J., Almeida, M.A., Santos, R., Bordado, J.M., Quinta-Ferreira, R.M., 2014. Compatibility  
32 analysis of municipal solid waste incineration residues and clay for producing lightweight  
33 aggregates. *Appl. Clay Sci.* 102, 71–80. doi:10.1016/j.clay.2014.10.016
- 34 Quina, M.J., Bordado, J.M., Quinta-Ferreira, R.M., 2014. Recycling of air pollution control residues  
35 from municipal solid waste incineration into lightweight aggregates. *Waste Manag.* 34, 430–8.  
36 doi:10.1016/j.wasman.2013.10.029
- 37 Rashid, R.A., Frantz, G.C., 1992. MSW Incinerator Ash as Aggregate in Concrete and Masonry. *J.*  
38 *Mater. Civ. Eng.* 4, 353–368. doi:10.1061/(ASCE)0899-1561(1992)4:4(353)
- 39 Schabbach, L.M., Andreola, F., Barbieri, L., Lancellotti, I., Karamanova, E., Ranguelov, B.,  
40 Karamanov, A., 2012. Post-treated incinerator bottom ash as alternative raw material for  
41 ceramic manufacturing. *J. Eur. Ceram. Soc.* 32, 2843–2852.

doi:10.1016/j.jeurceramsoc.2012.01.020

1  
2 Tan, W., Wang, L., Huang, C., Liu, Y., Green, J.E., Newport, D., Green, T., 2012. Utilization of  
3 municipal solid waste incineration fly ash in lightweight aggregates. *J. Cent. South Univ.* 19,  
4 835–841. doi:10.1007/s11771-012-1080-8  
5

6  
7 Verbinnen, B., Billen, P., Van Caneghem, J., Vandecasteele, C., 2016. Recycling of MSWI Bottom  
8 Ash: A Review of Chemical Barriers, Engineering Applications and Treatment Technologies.  
9 *Waste and Biomass Valorization* 1–14. doi:10.1007/s12649-016-9704-0  
10

11 Wiles, C.C., 1995. Municipal solid waste combustion ash : State of the knowledge. *J. Hazard. Mater.*  
12 3894, 20. doi:10.1016/0304-3894(95)00120-4  
13

14 Yeoh, A.K., Bidin, R., Chong, C.N., Tay, C.Y., 1979. The relationship between temperature and  
15 duration of burning of rice-husk in the development of amorphous rice-husk ash silica, in:  
16 *Proceedings of UNDP/ESCAP/ RCT, Follow-up Meeting on Rice-Husk Ash Cement.* Alor  
17 Setar, Malaysia.,  
18  
19  
20  
21  
22  
23  
24  
25  
26  
27  
28  
29  
30  
31  
32  
33  
34  
35  
36  
37  
38  
39  
40  
41  
42  
43  
44  
45  
46  
47  
48  
49  
50  
51  
52  
53  
54  
55  
56  
57  
58  
59  
60  
61  
62  
63  
64  
65

1  
2  
3  
4  
5  
6  
7  
8  
9  
10  
11  
12  
13  
14  
15  
16  
17  
18  
19  
20  
21  
22  
23  
24  
25  
26  
27  
28  
29  
30  
31  
32  
33  
34  
35  
36  
37  
38  
39  
40  
41  
42  
43  
44  
45  
46  
47  
48  
49  
50  
51  
52  
53  
54  
55  
56  
57  
58  
59  
60  
61  
62  
63  
64  
65

Table 1.- Formulation of unfired spherical pellets.

<b>WIBA – RH</b>	<b>(wt.% - wt.%)</b>				
	100 - 0	98 - 2	95 - 5	90 - 10	85 - 15

Table 2.- Chemical composition of the WIBA fraction >8 mm determined by XRF.

<b>Oxides</b>	<b>wt.% (dry basis)</b>	<b>Oxides</b>	<b>wt.% (dry basis)</b>
SiO <sub>2</sub>	53.15	K <sub>2</sub> O	1.56
CaO	15.14	SO <sub>3</sub>	0.87
Al <sub>2</sub> O <sub>3</sub>	6.46	TiO <sub>2</sub>	0.44
Na <sub>2</sub> O	5.43	P <sub>2</sub> O <sub>5</sub>	0.41
Fe <sub>2</sub> O <sub>3</sub>	4.28	MnO	0.07
MgO	2.01		
LOI*	9.58		

\*Loss on ignition at 1,000 °C.

1  
2  
3  
4  
5  
6  
7  
8  
9  
10  
11  
12  
13  
14  
15  
16  
17  
18  
19  
20  
21  
22  
23  
24  
25  
26  
27  
28  
29  
30  
31  
32  
33  
34  
35  
36  
37  
38  
39  
40  
41  
42  
43  
44  
45  
46  
47  
48  
49  
50  
51  
52  
53  
54  
55  
56  
57  
58  
59  
60  
61  
62  
63  
64  
65



Table 3.- Results from leaching test EN 12457-4.

	WIBA >8 mm (as received)	WIBA >8 mm (<80 µm)	LWA 0 wt.% RH	LWA 2 wt.% RH	LWA 5 wt.% RH	LWA 10 wt.% RH	LWA 15 wt.% RH	RL*
<b>pH</b>	9.06	9.34	7.70	7.65	7.74	7.73	7.95	
<b>Heavy Metals and Metalloids (mg·kg<sup>-1</sup>)</b>								
<b>As</b>	<0.01	<0.01	0.07	0.11	0.17	0.27	0.27	1.00
<b>Ba</b>	0.04	0.21	0.14	0.18	0.11	0.09	0.11	-
<b>Cd</b>	<0.01	<0.01	<0.01	<0.01	<0.01	<0.01	<0.01	1.00
<b>Cr</b>	0.10	0.13	0.62	0.64	0.29	0.15	<0.12	5.00
<b>Cu</b>	0.36	0.72	0.04	0.05	0.09	0.07	0.05	20.0
<b>Fe</b>	<0.10	<0.10	<0.10	<0.10	<0.10	<0.10	<0.10	-
<b>Hg</b>	<0.05	<0.05	<0.05	<0.05	<0.05	<0.05	<0.05	0.20
<b>Mn</b>	<0.01	<0.01	<0.01	<0.01	0.01	<0.01	<0.01	-
<b>Mo</b>	0.12	0.37	0.07	0.07	0.06	0.03	0.09	-
<b>Ni</b>	<0.02	<0.02	<0.02	<0.02	<0.02	<0.02	<0.02	5.00
<b>Pb</b>	<0.01	<0.01	<0.01	<0.01	0.07	0.04	0.03	5.00
<b>Se</b>	<0.10	<0.10	<0.10	<0.10	<0.10	<0.10	<0.10	-
<b>Sn</b>	<0.02	<0.02	<0.02	<0.02	<0.02	<0.02	<0.02	-
<b>Te</b>	<0.02	<0.02	<0.02	<0.02	<0.02	<0.02	<0.02	-
<b>Zn</b>	<0.10	<0.10	<0.10	<0.10	<0.10	<0.10	<0.10	20.0

\* Regulatory limit according to Catalan legislation (DOGC No. 2181; February, 15<sup>th</sup> 1996) for MSWI bottom ash reutilization.

## Figure Caption

1  
2  
3 Fig. 1. TGA and DTG of WIBA fraction  $> 8$  mm in air atmosphere ( $50 \text{ mL}\cdot\text{min}^{-1}$ ) with a heating rate  
4  
5 of  $10 \text{ }^\circ\text{C}\cdot\text{min}^{-1}$  up to  $1200 \text{ }^\circ\text{C}$ .  
6  
7

8  
9 Fig. 2. TGA and DTG of RH in air atmosphere ( $50 \text{ mL}\cdot\text{min}^{-1}$ ) with a heating rate of  $10 \text{ }^\circ\text{C}\cdot\text{min}^{-1}$  up  
10  
11 to  $1200 \text{ }^\circ\text{C}$ .  
12  
13

14  
15 Fig. 3. Image of the unfired LWA samples and fired spherical lightweight aggregates (after the  
16  
17 heating treatment). The expansion and shrinkage depending on the RH amount.  
18  
19

20  
21 Fig. 4. Weight loss after the sintering process at  $1100 \text{ }^\circ\text{C}$  for 5 min depending on RH percentage in  
22  
23 the formulation of the unfired pellets.  
24  
25

26  
27 Fig. 5. Optical images of fired LWA depending on the percentage of RH added as bloating agent. (a)  
28  
29 0 wt. %, (b) 2 wt. %, (c) 5 wt. %, (d) 10 wt.% and (e) 15 wt. %.  
30  
31

32  
33 Fig. 6. (a) Pore size distribution and (b) porosity of fired LWA depending on the percentage of RH  
34  
35 added as a bloating agent.  
36  
37

38  
39 Fig. 7. Volume shrinkage depending on the percentage of RH (wt.%) after the sintering process at  
40  
41  $1100 \text{ }^\circ\text{C}$  for 5 min.  
42  
43

44  
45 Fig. 8. (a) Apparent particle density and (b) water absorption of fired LWA depending on the  
46  
47 percentage of RH added as a bloating agent.  
48  
49

50  
51 Fig. 9. Compressive strength results for the sintered LWA based on the RH added.  
52  
53  
54  
55  
56  
57  
58  
59  
60  
61  
62  
63  
64  
65

1  
2  
3  
4  
5  
6  
7  
8  
9  
10  
11  
12  
13  
14  
15  
16  
17  
18  
19  
20  
21  
22  
23  
24  
25  
26  
27  
28  
29  
30  
31  
32  
33  
34  
35  
36  
37  
38  
39  
40  
41  
42  
43  
44  
45  
46  
47  
48  
49  
50  
51  
52  
53  
54  
55  
56  
57  
58  
59  
60  
61  
62  
63  
64  
65

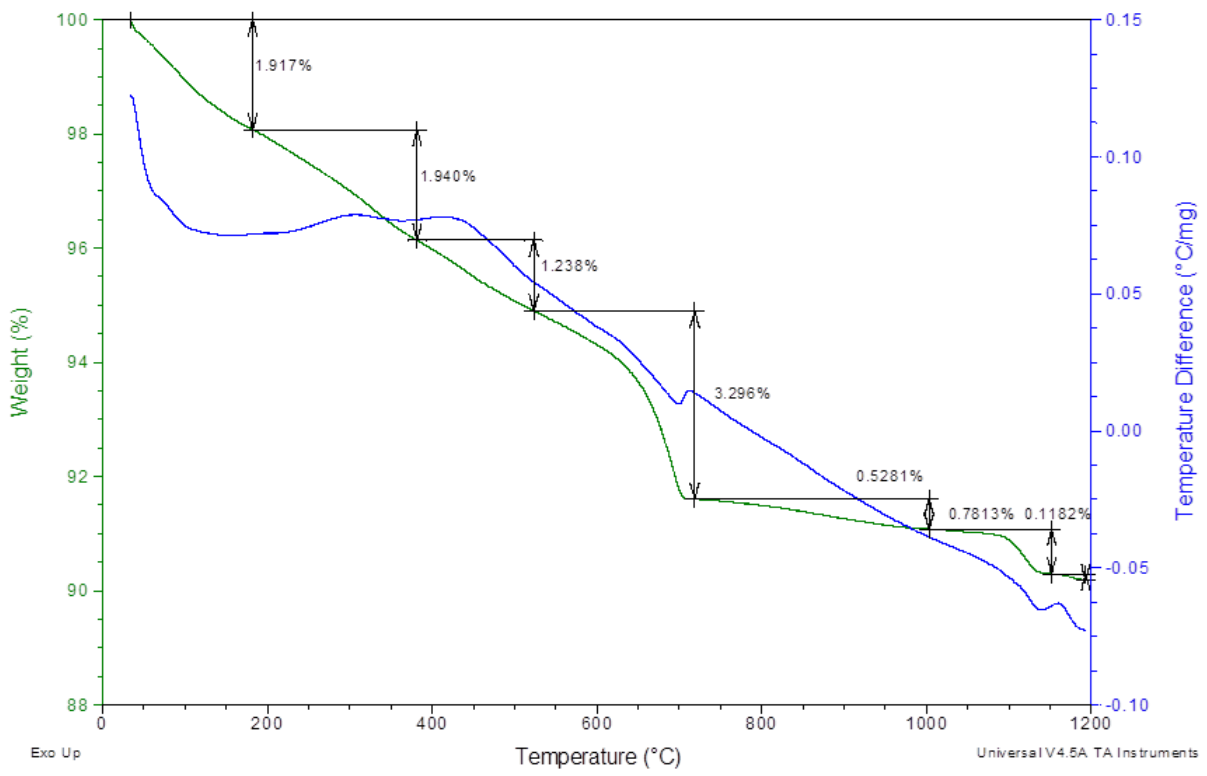


Fig. 1.

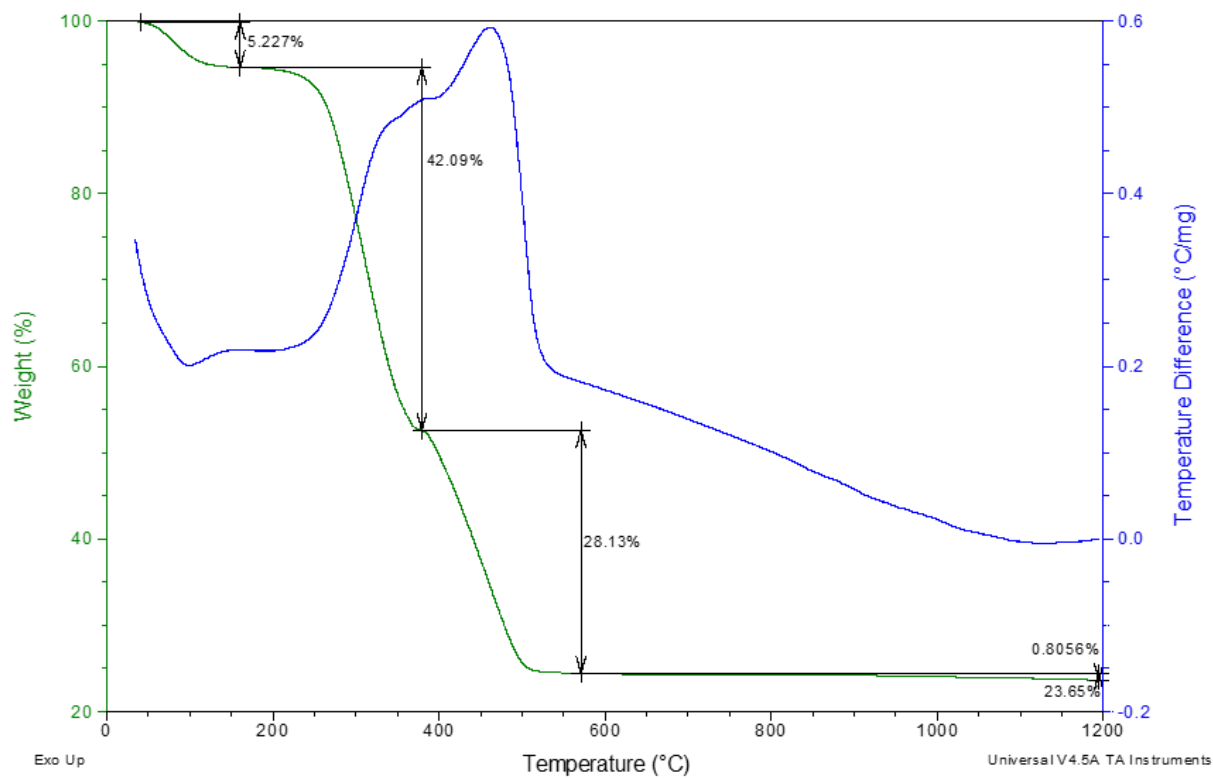


Fig. 2

1  
2  
3  
4  
5  
6  
7  
8  
9  
10  
11  
12  
13  
14  
15  
16  
17  
18  
19  
20  
21  
22  
23  
24  
25  
26  
27  
28  
29  
30  
31  
32  
33  
34  
35  
36  
37  
38  
39  
40  
41  
42  
43  
44  
45  
46  
47  
48  
49  
50  
51  
52  
53  
54  
55  
56  
57  
58  
59  
60  
61  
62  
63  
64  
65


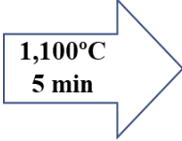



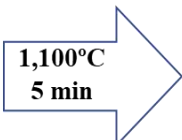


Unfired sample (10-12 mm)	Firing conditions	External appearance of LWA	Internal structure of LWA	Result after firing process
 95% WIBA + 5% RH	 1,100°C 5 min			<b>Expansion</b>
 85% WIBA + 15% RH	 1,100°C 5 min			<b>Shrinkage</b>

Fig. 3.

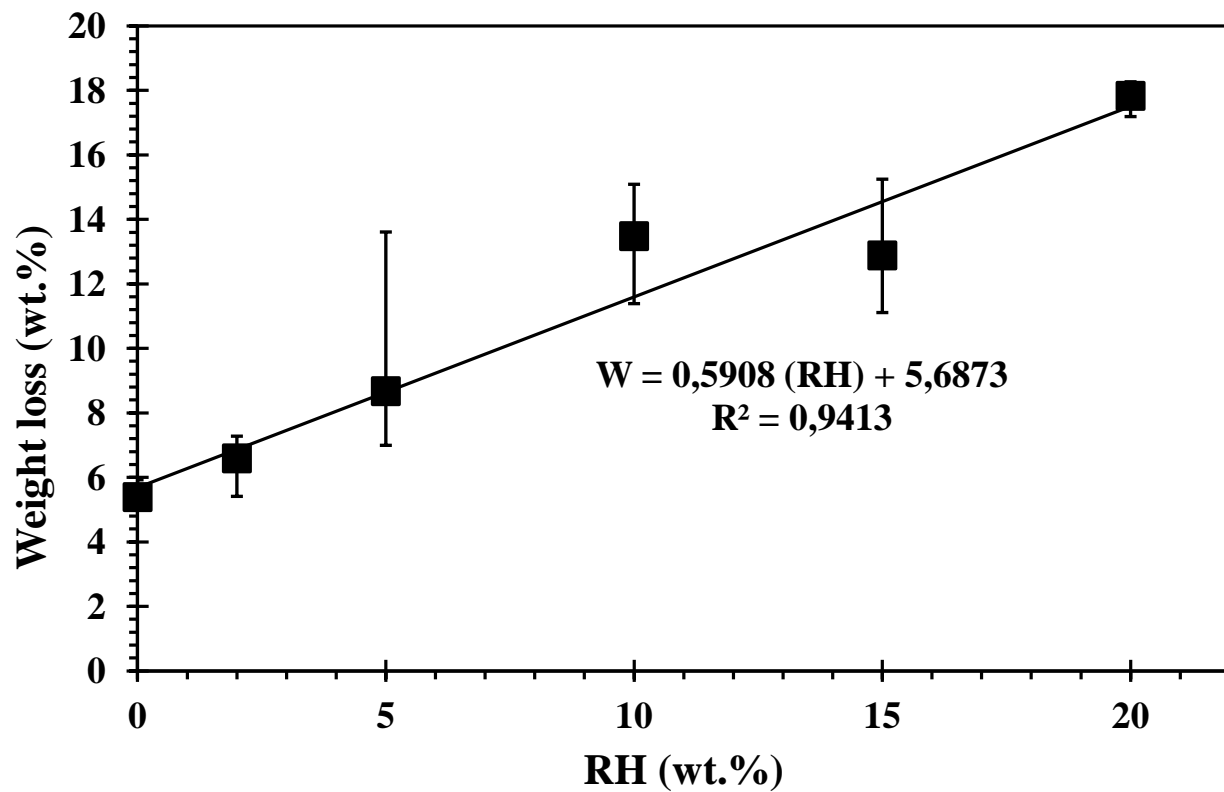


Fig. 4

1  
2  
3  
4  
5  
6  
7  
8  
9  
10  
11  
12  
13  
14  
15  
16  
17  
18  
19  
20  
21  
22  
23  
24  
25  
26  
27  
28  
29  
30  
31  
32  
33  
34  
35  
36  
37  
38  
39  
40  
41  
42  
43  
44  
45  
46  
47  
48  
49  
50  
51  
52  
53  
54  
55  
56  
57  
58  
59  
60  
61  
62  
63  
64  
65

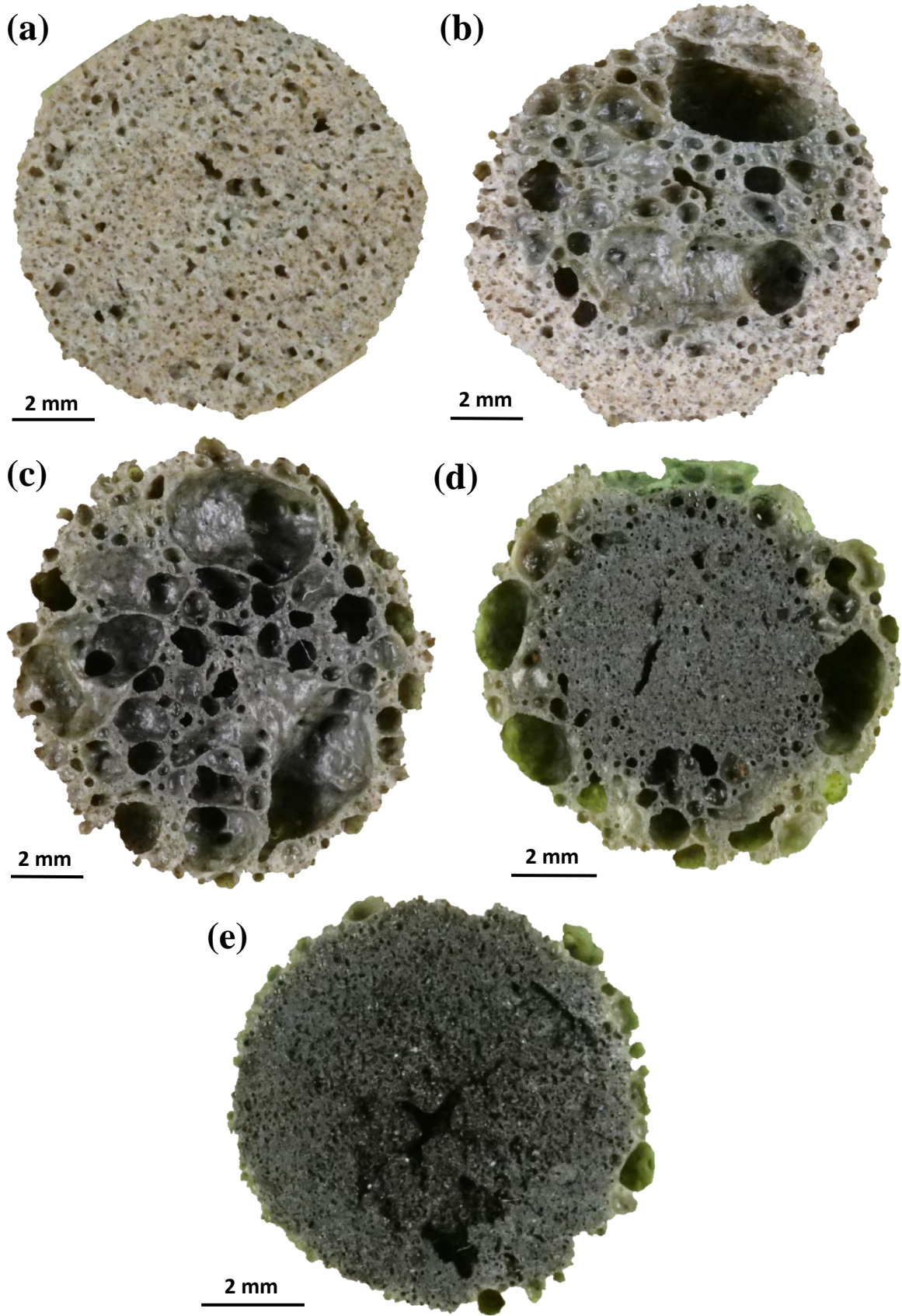


Fig. 5

1  
2  
3  
4  
5  
6  
7  
8  
9  
10  
11  
12  
13  
14  
15  
16  
17  
18  
19  
20  
21  
22  
23  
24  
25  
26  
27  
28  
29  
30  
31  
32  
33  
34  
35  
36  
37  
38  
39  
40  
41  
42  
43  
44  
45  
46  
47  
48  
49  
50  
51  
52  
53  
54  
55  
56  
57  
58  
59  
60  
61  
62  
63  
64  
65

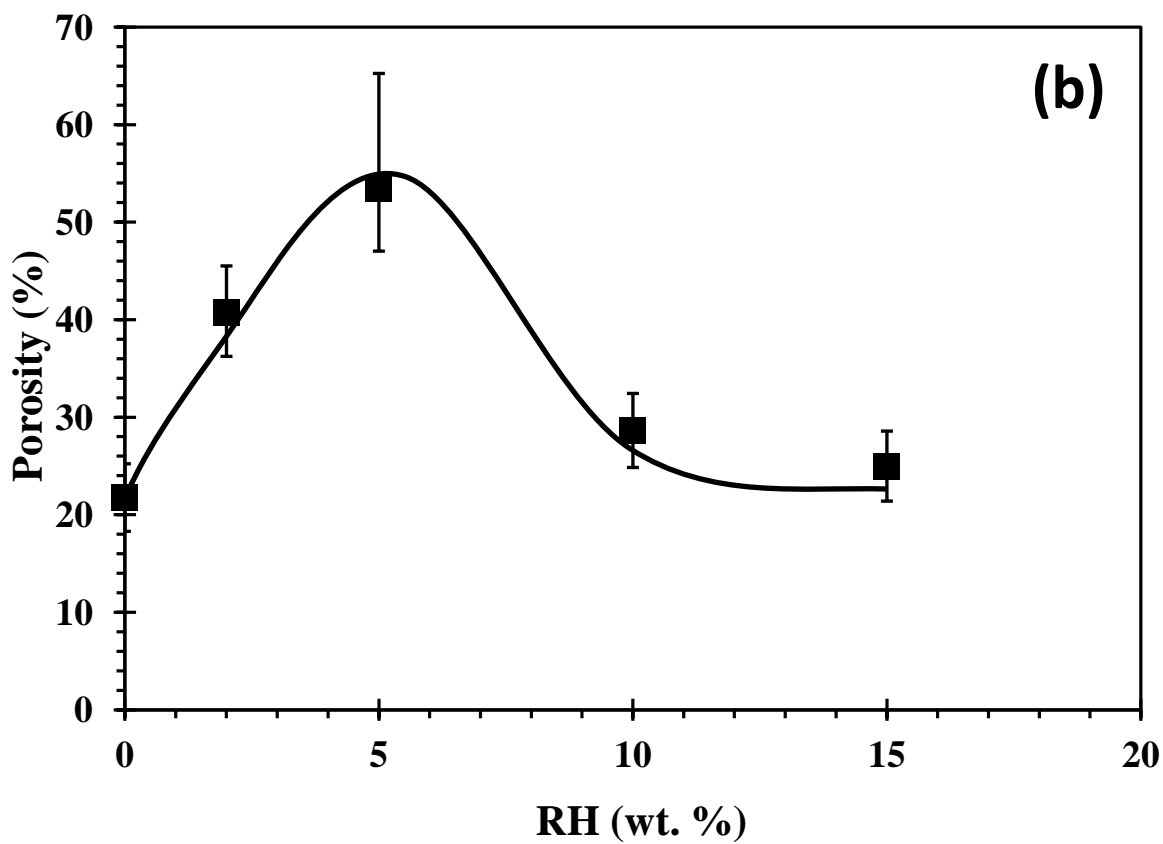
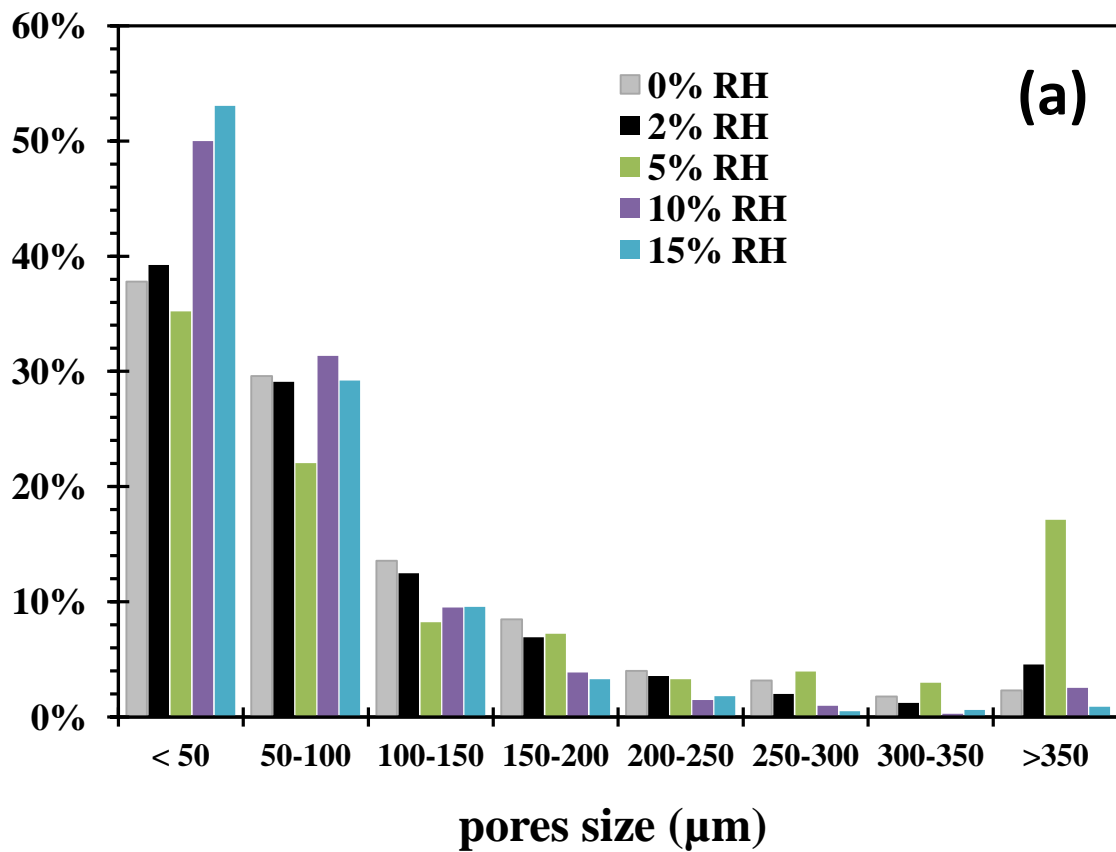


Fig. 6



1  
2  
3  
4  
5  
6  
7  
8  
9  
10  
11  
12  
13  
14  
15  
16  
17  
18  
19  
20  
21  
22  
23  
24  
25  
26  
27  
28  
29  
30  
31  
32  
33  
34  
35  
36  
37  
38  
39  
40  
41  
42  
43  
44  
45  
46  
47  
48  
49  
50  
51  
52  
53  
54  
55  
56  
57  
58  
59  
60  
61  
62  
63  
64  
65

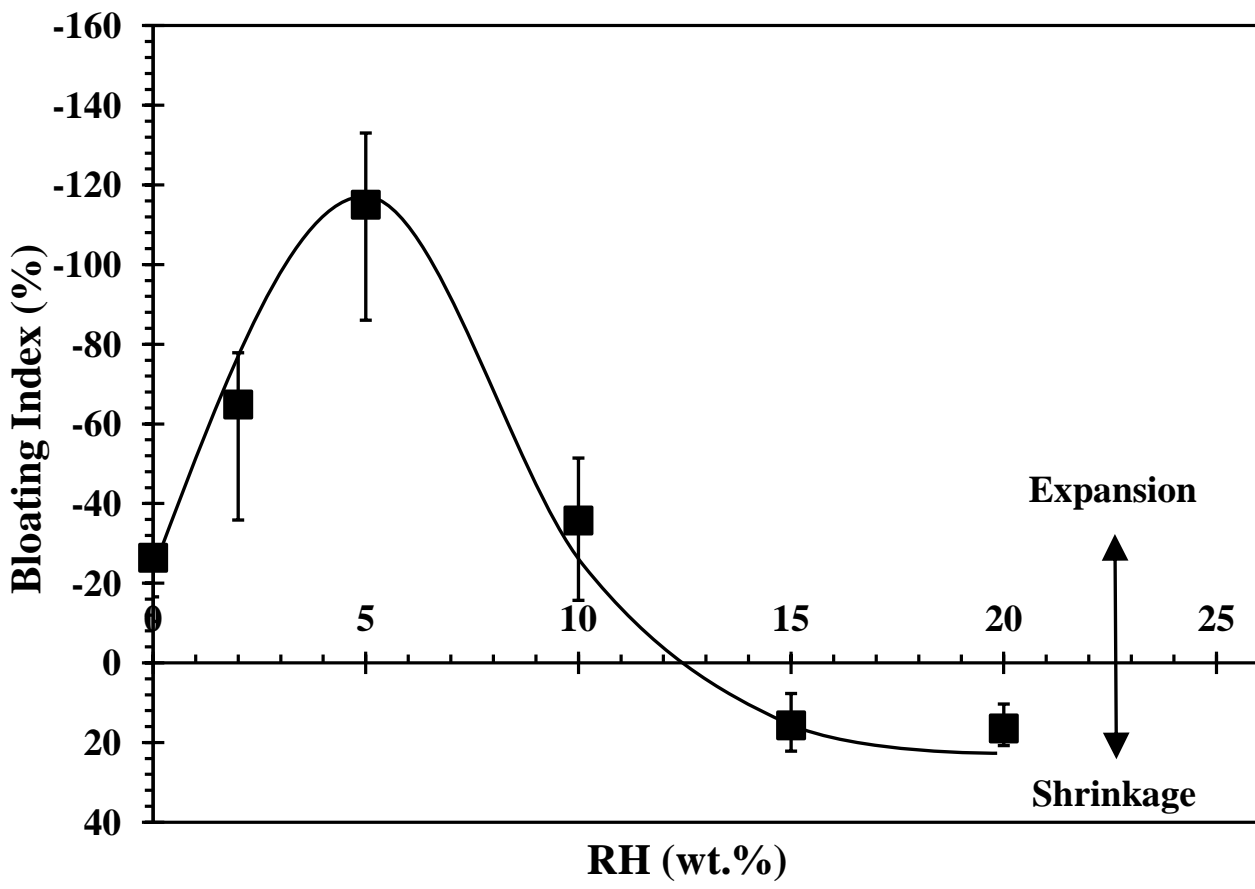
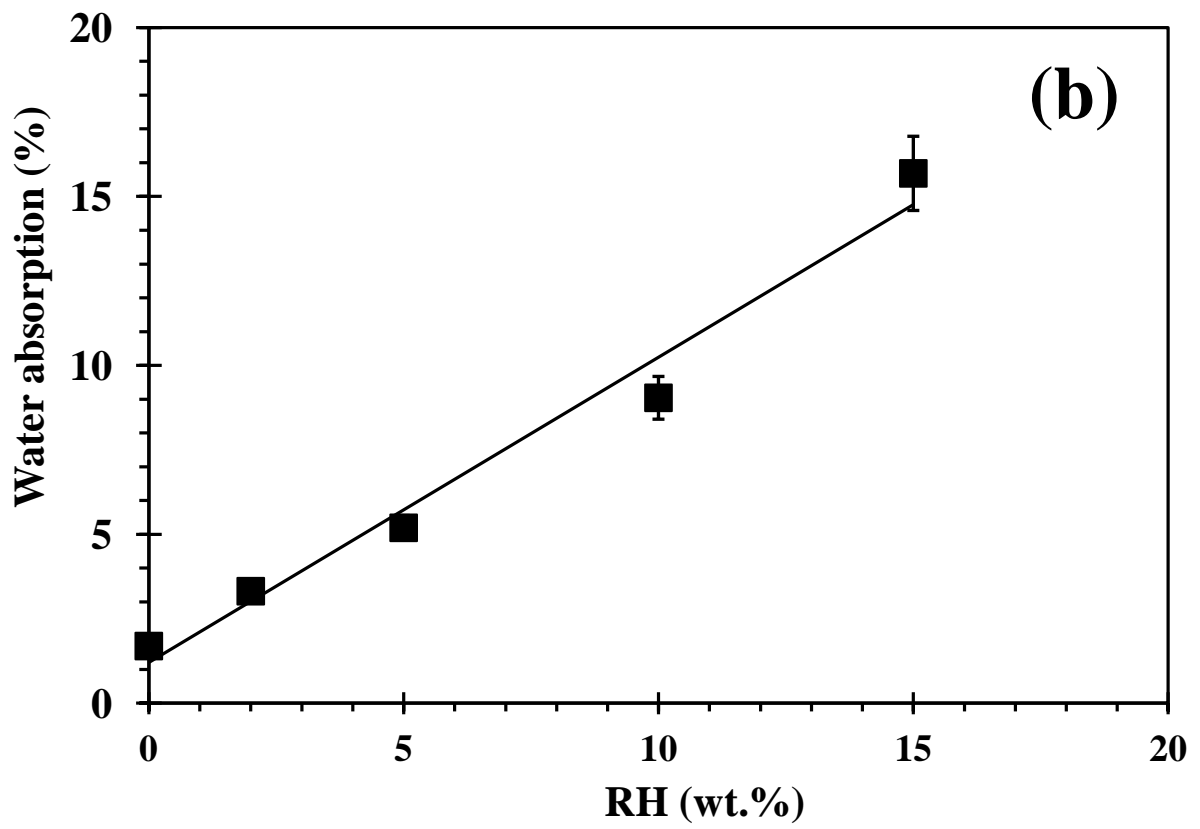
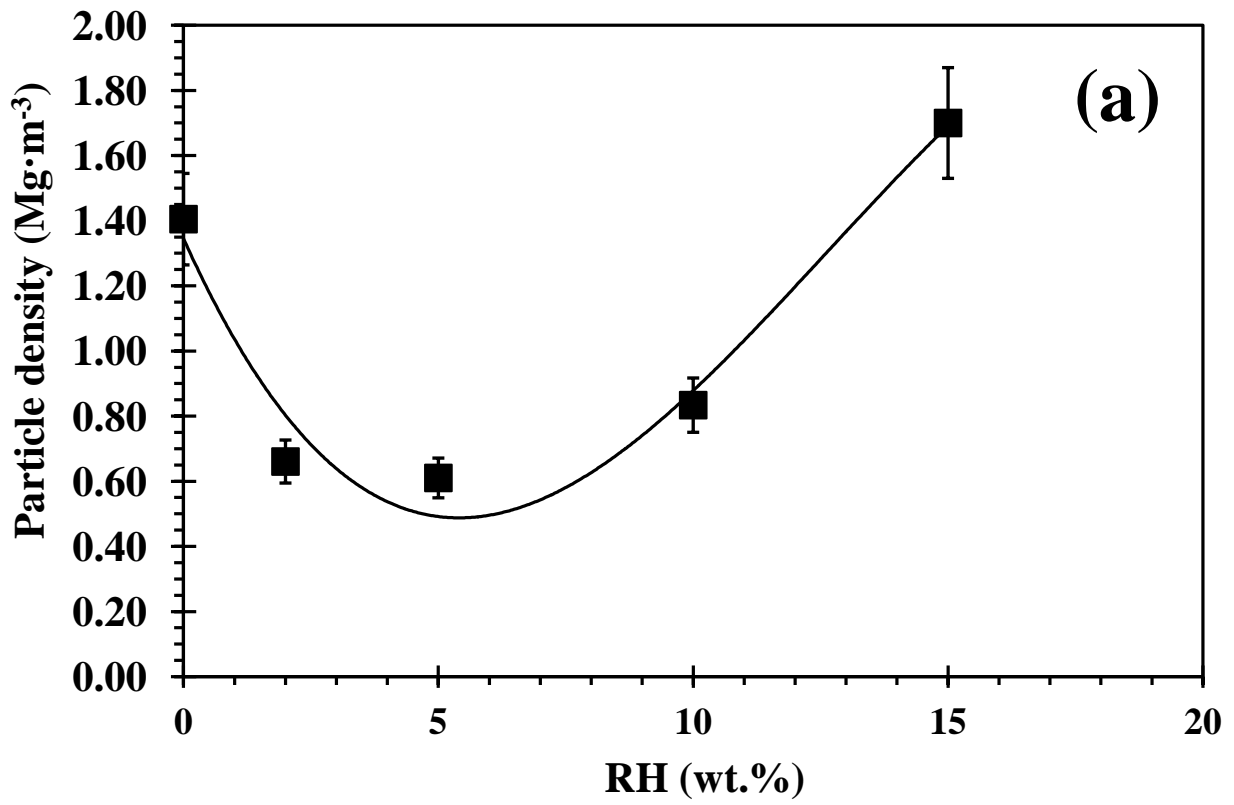


Fig. 7.



58 Fig. 8  
59  
60  
61  
62  
63  
64  
65

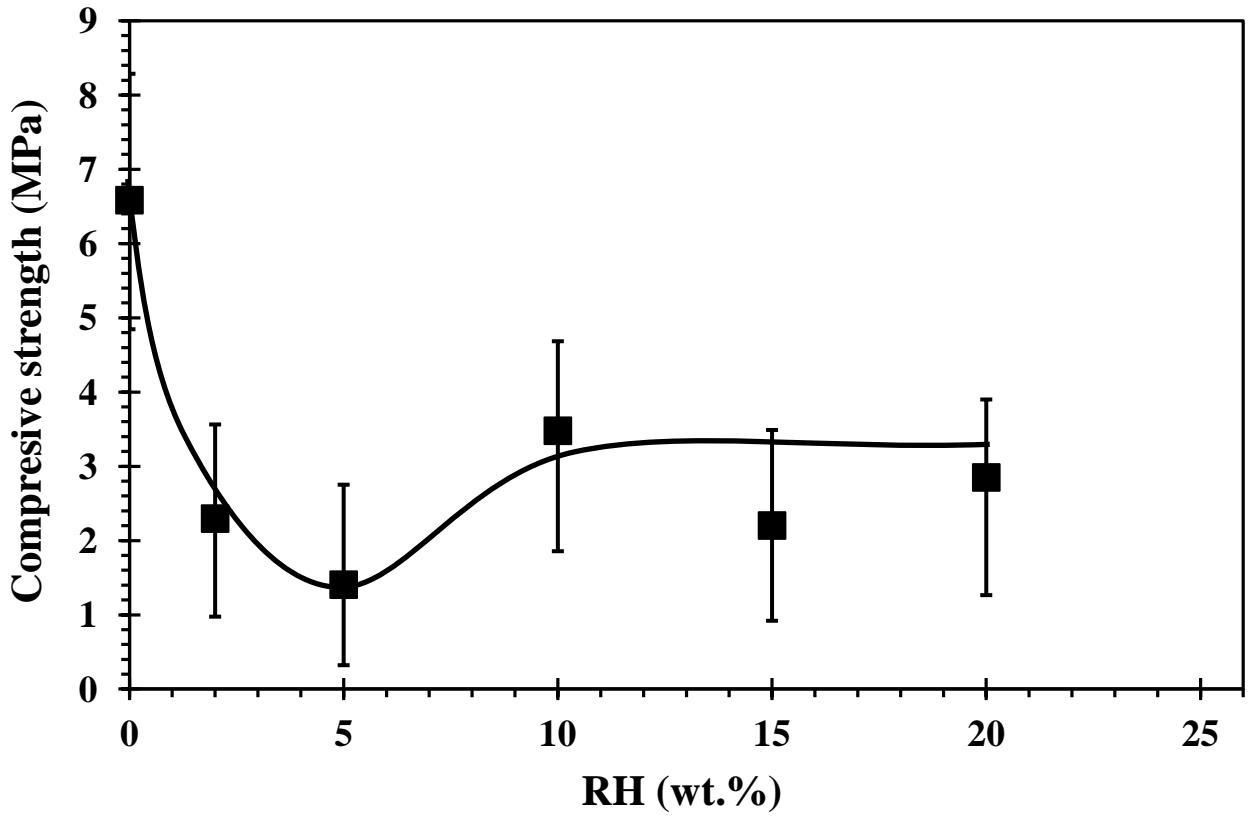


Fig. 9